Correlation of Atomic Roughness and Electronic Properties at the Si/SiO_2-Interface

Final Technical Report

by

Prof. Dr. M. H e n z l e r

Institut für Festkörperphysik
Universität Hannover, F. R. Germany

May 1988

United States Army
European Research Office

London England

Contract Number DA JA 45-85-C-0017
Prof. M. Henzler, Hannover

SECURITY CLASSIFICATION OF THIS PAGE (When Data Entered)

REPORT DOCUMENTATION PAGE

READ INSTRUCTIONS BEFORE COMPLETING FORM

1. REPORT NUMBER
2. GOVT ACCESSION NO.
3. RECIPIENT'S CATALOG NUMBER

4. TITLE (and Subtitle)
Correlation of Atomic Roughness and Electronic Properties at the Si/SiO_2 Interface

5. TYPE OF REPORT & PERIOD COVERED
Final Report
April 85 - May 88

6. PERFORMING ORG. REPORT NUMBER

7. AUTHOR(s)
Prof. M. Henzler

8. CONTRACT OR GRANT NUMBER(s)
DA JA 45-85-C-0017

9. PERFORMING ORGANIZATION NAME AND ADDRESS
Institut für Festkörperphysik
Universität, Appelstr. 2, 3000 Hannover

10. PROGRAM ELEMENT, PROJECT, TASK AREA & WORK UNIT NUMBERS

11. CONTROLLING OFFICE NAME AND ADDRESS

12. REPORT DATE
June 88

13. NUMBER OF PAGES

14. MONITORING AGENCY NAME & ADDRESS (if different from Controlling Office)

15. SECURITY CLASS. (of this report)

15a. DECLASSIFICATION/DOWNGRADING SCHEDULE

16. DISTRIBUTION STATEMENT (of this Report)

17. DISTRIBUTION STATEMENT (of the abstract entered in Block 20, if different from Report)

18. SUPPLEMENTARY NOTES

19. KEY WORDS (Continue on reverse side if necessary and identify by block number)
Si/SiO_2 interface, defects, in MOS devices, atomic steps, at interface, ESR at Si/SiO_2 interface electrical breakdown, correlation of defects, and electric properties, silicon, silicon dioxide, (high)

20. ABSTRACT (Continue on reverse side if necessary and identify by block number)
Scope: Investigation of steps and other defects at the Si/SiO_2 interface by spot profile analysis of LEED. Development of improved defect analysis by use of high resolution LEED systems. Search for correlations of defects with electronic properties of MOS-devices by measurement of defects and electrical properties on the same wafers.

Results: The development of the evaluation procedure makes use of a high precision measurement at many different energies: since the spot profile can be

DD FORM 1 JAN 73 1473 EDITION OF 1 NOV 65 IS OBSOLETE

SECURITY CLASSIFICATION OF THIS PAGE (When Data Entered)

separated in a central spike, two Lorentzian type shoulders and a constant background (which is not of interest here), the fraction of the contributions yields valuable informations: The central spike provides the vertical distribution (number of surface levels, distribution over the layers), the shoulders are used to derive the lateral width distribution of terraces and defect areas separately. Also the problem for analysis of the Si(100) has been solved. The Si(111) interface consists out of a 2-level structure, the Si(100) interface out of a 4-level structure. Annealing essentially reduces defect areas.
A comparative study on a set of Si(111) wafers with varying oxidation and annealing parameters includes defect analysis with high resolution LEED, optical stray light, ESR and electrical breakdown. It is demonstrated, that the defects are controlled by proper oxidation parameters and correlate well with the electrical data. Since high resistivity has been selected in favor of ESR, a new series has been prepared suited to include CV and radiation damage.

As a new feature for the first time regular step arrays have been identified at the interface close to the (111) orientation. The procedures have been checked to find the best regularity. This discovery opens the possibility to probe a new transistor type by making use of the minigaps due to the step array periodicity (Bloch oscillator).

Table of content

1. Publications and graduations

/1/ The $Si-SiO_2$ interface: Correlation of atomic structure and electrical properties
P.O. Hahn and M. Henzler, J. Vac. Sci. Techn. A2 (1984) 574

/2/ Defects at semiconductor surfaces
M. Henzler, Surf. Sci. 152/153 (1985) 963.
Invited talk at ECOSS 84 in York, England

/3/ Microstructure and Electronic properties of $Si-SiO_2$ Interfaces, M. Henzler in "Insulating films on Semiconductors" Eds. J. J. Simonne and J. Buxo, North Holland 1986. Invited talk on INFOS 85, Toulouse.

/4/ Quantitative Evaluation of Terrace width Distributions from LEED Measurements
H. Busch and M. Henzler, Surf. Sci. 167 (1986) 534

/5/ The Microstructure of the Si/SiO_2 interface: observation and related electronic properties
M. Henzler in Inst. Phys. Conf. Ser. 82 (1986) 39.
Invited talk at ESSDERC 86, Cambridge, England

/6/ A New LEED instrument for Quantitative Spot Profile Analysis, U. Scheithauer, G. Meyer, M. Henzler, Surf. Sci. 178 (1986) 441

/7/ The Microstructure of Technologically Important Silicon Surfaces
M. Henzler, in Advances in Sol.St.Physics 27, p 185
Ed. P. Grosse, Vieweg 1987
Invited talk at the General Meeting of the German Physical Society

/8/ Nucleation and Growth During MBE of Si on Si(111)
R. Altsinger, H. Busch, M. Horn, M. Henzler
Surf. Sci. (1988) in press

/9/ The rms-Roughness at the $Si(111)/SiO_2$ interface
J. Wollschläger, M. Henzler, in preparation

Graduations: PhD P. Marienhoff, 1988

Diploma J. Wollschläger, 1986
O. Jusko, 1988

2. Introduction and Survey of results

The steady increase of large scale integration requires smaller and smaller structures with thinner and thinner layers. Simultaneously the number of defects has to be decreased so that any kind of defect analysis is very important for improvement of the production of devices. One key issue is the quality of the Si/SiO_2 interface. Our own results of the recent years have demonstrated, that defects at the interface are identified and quantitatively measured by spot profile analysis of LEED. Whereas TEM and XPS provide also some qualitative and only limited quantitative results, only LEED was so far able so measure systematic variations of atomic roughness at the interface due to variation of oxidation parameters (see our final report DA JA 37-81-C-0054 and references /1/ and /2/). Additionally a direct correlation of atomic roughness to electronic properties like mobility and interface state density could be shown.

The purpose of the present investigation has been, to analyze the atomic roughness at the interface in more detail, so that the quantitative description is more complete. The investigations should be expanded from Si(111) to the technologically more important Si(100) which is more complicated due to the equidistant sublattices of the diamond lattice in the [100] direction. With the better structural information a more detailed correlation to electrical data like mobility, ESR and radiation damage should be possible. The maximum field strength for electrical breakdown should be related to atomic roughness too.
The results have been obtained in part by LEED investigations in our laboratory. Those studies have been very successful and have a lot of results not even expected in the proposal. For the comparative studies we needed outside help for obtaining oxidation and electrical measurements with commercial standard. Those measurements were badly delayed for reasons we could not influence, so that this part of the proposal is only fulfilled in part, it is to be continued, until the missing measurements are completely added.

The results will be described according to the main aspect of each special study.

3. Development of Roughness Analysis

Since in this study for the first time the newly developed high resolution LEED system has been used, it was necessary to develop the evaluation procedures, so that the improved set of data is used not only for a higher accuracy (a factor of up to 20 has been obtained). It has been rather desirable to find also new kind of informations not yet available so far.

3.1 Terrace width probability distribution

Up to now only fitting procedures have been used to determine the probability distribution. Here just a distribution had to be assumed, then the autocorrelation and its Fourier transform was constructed and compared with a measured profile (see ref. /2/). So by trial and error a best fit was approximated. A straightforward derivation has been found in ref. /4/, which provides a direct transform of the spot profile into a probability distribution. The details are found in ref. /4/. As a first success for the first time it could be shown, that the contribution of the background to the profile is of decisive influence onto the quantitative evaluation (ref. /4/).

3.2 Vertical structure

So far only the lateral structure could be derived out of the spot profile . The high resolution profiles, however, showed, that in most cases the profile consists out of a central sharp spike and a well separated broad shoulder /6/. It could be demonstrated, that the fraction of intensity in the spike out of the integrated spot intensity varies characteristically with energy. This variation is easily described within the kinematic approximation and contains just the vertical probabilities (the probability of finding a surface atom at a given vertical level). Consequently it is now for the first time possible to derive those probabilities (at least their autocorrelation) /6/. If a small number of levels is involved or if a symmetric distribution is assumed, a unique evaluation is possible, which enables an excellent atomic view of surface structure. The details of analysis, its experimental proof and its application to MBE is found in ref. /6/.

3.3 RMS-Deviation from average surface

If all vertical probabilities p_i are known, the rms-roughness σ is easily derived

$$\sigma^2 = \Sigma\, p_i\, i^2 - \Sigma\, (p_i \cdot i)^2$$

Due to ambiguity for p_i data at a large number of layers it is desirable to have a direct and model independant determination of the rms-roughness. Such a determination is possible with the energy dependence of the function G(K), which is the above function to describe the fraction of the integral peak intensity within the central spike. If the function G(K) is represented by its Taylor expansion at an

in-phase-condition, already the second coefficient provides the roughness Δ

$$G(K) \approx 1 - \Delta^2 K^2$$

Since the experiment yields directly the roughness out of the curvature, the determination is completely independent of any model or assumption /9/. Additionally the roughness Δ and the correlation L are the quantities needed to describe the mobility due to roughness scattering quantitatively. Since both quantities are directly derived out of the LEED measurement, the comparison of mobility and roughness is now possible without fitting parameter.

3.4 Chemical inhomogenities

It is well known, that any defect, structural or chemical, may produce a broadening of a spot profile. The defects due to steps are easily separated by the periodic variation of the profile with energy (/1-3/). It is desirable, to know simultaneously any other defects at the surface. A general concept has been recently developed with the inclusion of two different formfactors, which besides steps also gives rise to a shoulder (completely described in the diploma thesis of J. Falta (1988), to be published soon). This procedure has been used to distinguish at the SiO_2/Si interface between steps and other defects, which will be discussed in the next chapter (see also /9/).

4. The Annealing of the SiO_2/Si(111) interface

4.1 Experimental results

Commercially polished Si(111) wafers have been oxidized in dry oxygen at 800°C until a 10 nm thick oxide has been grown. Some wafers have been annealed in nitrogen at 800°C or 1000°C for different periods of times. The purpose has been to determine defects with high resolution and to measure changes due to annealing.

As developed in earlier studies /1/ the oxide has been removed in HF and transferred under a droplet of methanol into the ultrahigh vacuum, so that a reoxidation in air could be avoided. The high resolution SPA-LEED was similar to that described in /6/. Due to the high transfer width of more than 100 nm (at least 5 times better than in earlier studies of ref. /1/ and to the high dynamic range of 5 orders of magnitude quite a few informations have been

obtained, which are qualitatively and quantitatively far beyond the earlier studies.

The spot profiles have been measured along the reciprocal lattice(00)-rod between the 555 and 666 Bragg spots, that is between 90 and 140 eV, so that the phase varies between $5 < S < 6$ with $2\pi.S$ the phase shift of scattering at adjacent levels. The spot profile at the out-of-phase condition ($S = 5.5$) is shown in fig. 4.1 for the not-annealed wafer. For comparison purposes also as a solid line the profile is shown for a well annealed surface, which reproduces the instrumental resolution. The difference of the two curves, which after two-dimensional integration is much higher than the central spike, shows the broadening due to defects. For quantitative evaluation the measured profile is fitted by a sum out of four components: the central spike (given by a δ-function convoluted with the instrument response function), two Lorentzian profiles with different half widths and a constant background.

The four contributions are found by a logarithmic plot of the out-of-phase pair correlation, which is the fourier transform of the measured profile. Whereas background and central spike are separated by the pair correlation value at zero and the values at high distances (more than some hundred atomic distances), the two Lorentzians are now available as linear portions of the pair correlation. Whereas the constant background is not further discussed as being due to thermal diffuse scattering or random distributed point defects, the other three ones are studied carefully by measurement at many different energies. Fig. 4.2 shows the spot profile of the same sample as in fig. 4.1 here for in-phase-condition ($S = 5.0$). It is easily seen, that the profile consists not just of a central spike (and a constant background), one broad Lorentzian has to be added. By comparison with fig. 4.1 it is found, that the same broad shoulder persists, only the small Lorentzian shoulder of fig. 4.1 is gone. It is therefore concluded that the small shoulder is due to steps and the broad shoulder due to other defects. For a clear distinction and quantitative evaluation the integral contributions of the three components (neglecting the background) are measured relative to their total intensity. The results are shown in fig. 4.3 with the contribution I_S of the narrow Lorentzian shoulder and I_B of the broad Lorentzian shoulder. The shape has been except scaling identical for all samples, so that an evaluation is consistently possible. The broad shoulder does not disappear for in-phase-condition, it is therefore due to defects, described by a different form factor f_2 (as explained in chapter 3). It is described for most energies within the approximation of a very small form factor of the defect areas, so that a constant value for I_B is obtained for most of the energies. Only close to $S = 5.5$ larger values are obtained. Here the intensity for the clean silicon is very low, so that the approximation $f_1 >> f_2$ does

no more hold. The deviation is therefore understood. The constant value is used to derive the coverage of the surface with defect areas of low form factor, because its value is directy the coverage Θ_b with different formfactor f_2.

The narrow shoulder shows a nearly sinusoidal variation with energy, which is characteristic for a two-level stepped surface. For a quantitative evaluation not its contribution to the total integrated intensity is useful, according to the theory, rather its contribution to the sum out of central spike and narrow shoulder should be used. Fig. 4. 4 shows its complement, that is the integral of the central spike over the sum out of this spike and the narrow shoulder, which reproduces the sinusoidal shape to a more large extent. This function is evaluated according ref. 8 as a perfect two-level-system with a coverage in one level of about 35 %. (see table 1). The rms roughness as explained in chapter 3 is also shown in table 1.

The lateral distribution of both steps and the other defects is derived out of the shape and width of the profiles. Since both profiles have exactly a Lorentzian shape, their pair correlation is given by an exponential function. Therefore the length or size distribution is given by the geometric distribution

$$P(\Gamma) = \frac{1}{\langle\Gamma\rangle}\left(1 - \frac{1}{\langle\Gamma\rangle}\right)^{\Gamma - 1}$$

where $P(\Gamma)$ is the probability of finding a terrace or domain of width Γ (in multiples of the lattice constant a). Just one parameter, the average width $\langle\Gamma\rangle$ is sufficient for description of the length distribution for each entity (lower or upper level, defect free or distorted areas). The shoulder in a one dimensional description is given by the function

$$G_D\left(K_{\parallel}, K_{\perp}\right) = \frac{1 - \beta}{1 + \beta} \cdot \frac{4\,\Theta\,(1 - \Theta)\,\sin^2\,(K_{\perp} d/2)}{1 + \beta^2 - 2\,\beta\,\cos\,(K_{\parallel}\,a)}$$

which may be described by a sum of identical Lorentzians at each position of a diffraction spot. The parameter β describes the expontential decrease of the pair correlation $\phi(n) = \exp(-n/\xi)$ via a correlation length

$$\xi = -\frac{a}{\ln \beta}$$

The coverage Θ as derived above, and the parameter β provide the average width $\langle \Gamma_0 \rangle$ and $\langle \Gamma_1 \rangle$ for the two levels or the two kind of surface patches

$$\langle \Gamma_0 \rangle = (\Theta \quad (1 - \beta))^{-1}$$

$$\langle \Gamma_1 \rangle = ((1 - \Theta) \quad (1 - \beta))^{-1}$$

Those numbers are shown in table 4.1 and 4.2.

4.2 Discussion

The results summarized in table 4.1 and 4.2 show, that the interface is extremely smooth. The roughness is given by about half the layer distance. Only a change between two levels along the interface is observed. The average terrace width, as derived out of the energy dependent shoulder is fairly large. Both the roughness and the terrace width are nearly not affected by heat treatment.

An independent and completely new information is derived out of the broad shoulder with the nearly energy independent amplitude. It is concluded that at the surface only part of the surface consists of well ordered, clean silicon (the percentage is given in table 2, as derived out of the intensity of the broad shoulder at energies close to the in-phase condition). The rest of the surface is covered with domains of different, for most energies much lower form factor. Those domains again have a size and distance distribution as given by the geometric distribution. Therefore their average length can be given in table 2.

Possible origins for those domains of low scattering power (or form factor) are discussed now. It may be due to areas with different chemical composition. It has been shown, that a fraction of a monolayer of oxygen and carbon is found at those surface. On the other hand structural disorder in some areas may work the same way. It may be a combination of the two, that oxygen, embedded a little bit deeper during oxidation produces some structural disorder. The large half width of the shoulder means, that those distorted areas are fairly small, only 3 to 8 atomic distances in average. The distribution again is geometric, pointing to a random process of generation without correlation. In big contrast to the step structure the average domain size and the coverage with domains is drastically changed by annealing. So it is likely, that during oxidation some defects at the interface are generated, which to some extent may be annealed in nitrogen.

posttreatment of the $Si(111)/SiO_2$-interface	none	800 °C 10 min	1000 °C 10 min	1000 °C 60 min
coverage of the top-layer Θ [% of ML]	36 ± 6	34 ± 7	31 ± 11	36 ± 5
asperity height Δ [Å]	1.51 ± 0.06	1.48 ± 0.06	1.44 ± 0.16	1.51 ± 0.03
terrace correlation length [nm]	6.5 ± 0.7	6.5 ± 0.7	6.5 ± 0.7	6.5 ± 0.7
average terrace length of the bottom-layer [nm]	19 ± 5	20 ± 6	22 ± 10	19 ± 4
average terrace length of the top-layer [nm]	10 ± 2	10 ± 2	10 ± 3	10 ± 2
step atom density [%]	2.3 ± 0.4	2.2 ± 0.4	2.1 ± 0.6	2.3 ± 0.4

Table 4.1

posttreatment of the $Si(111)/SiO_2$-interface	none	800 °C 10 min	1000 °C 10 min	1000 °C 60 min
silicon coverage Θ_{Si} [% of ML]	87 ± 2	76 ± 5	85 ± 5	95 ± 2
domain correlation length [nm]	1.16 ± 0.05	1.34 ± 0.07	1.91 ± 0.13	2.60 ± 0.23
average length of the silicon domains [nm]	10 ± 2	6 ± 2	14 ± 5	57 ± 27
average length of the defect domains [nm]	1.5 ± 0.1	1.8 ± 0.2	2.5 ± 0.3	2.9 ± 0.3
defect domain density [%]	2.8 ± 0.5	4.1 ± 0.8	2.0 ± 0.7	0.6 ± 0.2

Table 4.2

In earlier experiments with low resolution instruments a distinction between the two types of defects were not possible. Therefore the reported annealing effect on half width at the out-of-phase condition (S = 5.5) may be just the annealing of the defects.

The influence of the two types of defects (steps and inhomogeneities) on electrical properties so far only can be guessed /1/. The reported effect on mobility may be due to both types of defects. It has been reported, that the interface state density, which smaller that the step atom density by orders of magnitude, varies also with the half width. Here it is more likely, that the inhomogeneities are the origin of the sites for fixed charge. For a clear conclusion dedicated experiments are needed. So far, however, it is already shown, that two different types of defects may be separated experimentally, so that a direct correlation to electrical properties may be studied in detail.

5. The SiO_2/Si(100) interface

The Si(100) surface has for electron diffraction the disadvantage, that subsequent layers belong to different sublattices and are therefore not equivalent. The interference pattern may be modified by different scattering factors, up to the limit of very different form factors with a misinterpretation of double steps. Since the two levels are identical after a rotation of 90°, the form factors are identical, if the incident beam is selectd with an azimuthal direction just 45° to the two levels. To check the influence of different form factors onto the intensity for the central spike, a four level system (with all levels at same probabiliy has been calculated for a variing ratio of the two form factors (fig. 5.1). It is seen, that the central spike is not affected for energies close to an in-phase-condition. Therefore the analysis for rms roughness is not affected. Whereas at out-of-phase for very different form factors (the ratio A of the form factors A = 0.0) the high central spike might look like in a double step structure, already a factor of 0.5 brings the relative peak intensity down to about 10 %. It is therefore important to choose a diffraction condition, so that both levels contribute.

Samples have been oxidized and annealed the same way as the (111) samples (10 nm oxide in dry oxygen, increasing anneal in nitrogen). A result is shown in fig. 5.2 . It is seen in the upper half (direction for equivalent levels), that four levels are needed for description with approximately the same probability for each level. Close to out-of-phase condition no central spike was observed, which may

T a b l e 5.1

posttreatment of the $Si(100)/SiO_2$-interface	none	800°C 10 min	1000°C 10 min	1000°C 60 min
terrace correlation length (nm)	7.7	12.7	12.7	19.2
domain correlation length (nm)	12.3	13.8	16.5	23.8
roughness (nm)	0.18	0.18	0.18	0.18
number of levels	4	4	4	4

be also due to a vanishing form factor. It is more likely, however, that it is due to destructive interference. If the azimuth of the incident beam is changed by 45° degrees, the form factors of the two levels are quite different, so that at out-of-phase condition a large central spike is seen. Since that difference is known, nevertheless the four levels are to be taken for description.

The evaluation has been done the same way as with the Si(111) samples (table 3).

The central spike provides the roughness (always 1.8 A) and the number of layers (always 4). The spot profile again consists of a narrow Lorentzian shoulder (steps) and a broad Lorentzian shoulder (inhomogeneities), which are given in the table with the respective average widths. Since the data have not been collectd for a number of energies as high as with the (111) samples, the interpretation of the broad shoulder as due to inhomogeneities is just done analogous to the (111) surface.

Since the step height at the (100) surface is only 1.34 Å (compared to 3.13 Å at (111)), the rms roughness of 1.8 Å over 4 layers may yield a smoother surface on an atomic scale than the (111) surface (with rms roughness of 1.5 Å). At the (100) interface the annealing both reduces the step density and the inhomogeneity distribution which is in contrast to the (111) results, reported above.

The present results provide the first detailed description of the SiO_2/Si(100) interface. In TEM studies mostly only two levels are seen, since the resolution is only close to 1.7 Å. The present result has the same good interfaces, it resolves, however, due to the much better resolution, all four levels, which contribute to the formation of the interface.

6. Regular Step arrays at the SiO_2/Si(111) interface

A set of wafers was misoriented away from the (111) direction by 1.7°. For a perfect interface a regular step array with a terrace width of about 100 A is expected. It has been assumed, however, that the interface roughness should obscur the regular array completely. Since some of the wafers have been carefully annealed after oxidation, it was of interest if any regularity would be visible.

Fig. 6.1 shows a clear splitting of the spot, which is quantitatively resolved in fig. 6.2 for a linear scan. The clear splitting shows a good regularity, which is improved by annealing. Since the same wafers have been used for the comparative study (see section 7), here only the aspect of regular step array is discussed.

Here for the first time a regular step array has been detected at the Si/SiO_2 interface. The broadening of the double spot and broad base (which is important even after notice of the logarithmic scale in fig. 6.2) shows deviations from the regularity. For description of those irregularities appropriate parameters or measures had to be found. For that purpose first a functional form for the terrace width distribution had to be detected. The selected function has to reproduce the correct spot profile not only for out-of-phase condition (fig. 6.2), the profiles at all other energies have to fit automatically.

After several attempts a special function, which is derived out of the geometric distribution, provided an excellent fit. The Gamma distribution $P(\Gamma) = \Gamma^a \exp(-\Gamma/r)$ provides the fit as is shown in fig. 6.2. The distribution is shown in fig. 6.3, where the parameters a and r have been selected so that in all cases the average terrace width (and therefore the splitting of fig. 6.2) is the same. The sharper the distribution, the deeper is the minimum between the split spots. To reduce the number of parameters, only two are used for further description. One is the average terrace width, which for a monotonuous step array is given by the angle of misorientation. The other one is the standard deviation σ from the regular step array with the average terrace width. For an ideally regular array it would be zero. In reality the terrace width varies, so that the standard deviation is a measure of irregularity.

For the direction parallel of the step edges the profile is identical to those found on well oriented wafers. Therefore the same fitting procedure and the same parameters may be used: the rms roughness, the average length of an excursion into the next level. For the stepped surface the second parameter may also be expressed as the average length of straight portions (free of kinks) along the step edge direction.

Therefore the LEED evaluation provides detailed information on the deviations from regularity. All investigated samples had the same misorientation, they had, however, due to different oxidation parameters quite different standard deviations from regularity and average length of straight edges. The results will be discussed in section 7 together with the electrical and optical properties of the same wafers.

Here only the importance with respect to possible electrical transport properties due to the new periodicity should be discussed. Any new periodicity produces new Brillouin zone boundaries and therefore new forbidden gaps in the band structure (minigaps and minibands). If th mean free path is much larger than the new period (10 nm in this case) the carriers no more move in the parabolic part of the

conduction band, close to the minigaps drastic anomalies in conductivity are expected, which may be used for a new transistor concept (Bloch-transistor). The present experiments show, that it is possible to produce a regular step array at the Si/SiO_2 interface. The regularity may be varied to a large extent by appropriate oxidation parameters. It would be worthwile to check directly for those transport anomalies in new experiments.

7. Comparative Study with many methods

7.1 Samples and preparation

A set of wafers Si(111) has been oxidized in 6 groups with 4 wafers each with variation of parameters, which are shown in the following table 7.1.

T a b l e 7.1

Group	I	II	III	IV	V	VI
preoxidation (thick oxide)	x	x	x	x	-	-
oxidation in dry O_2 (thickness in nm)	40	40	90	90	40	-
wet-dry	-	-	-	-	-	100
annealing in dry N_2 (1 hr, 1000°C)	-	x	x	-	x	x
optical light scattering						
before oxidation	all lower than 6					
after oxidation (% of max. value)	70	70	26	26	11	100

The set of parameters was selected to obtain informations on the effect of the following parameters:

a) influence of preoxidation (group II and V)
b) influence of oxide thickness (I - IV, II - III)
c) influence of annealing in dry N_2 (I - II, IV - III)
d) influence of wet oxidation (VI - III)

The samples have been selected with high resistivity and polished on both sides, so that ESR was possible. The preoxidation was on oxide of 100 nm and an anneal in N_2 at 1000°C for 1 hr. This oxide has been removed in HF before the next oxidation was started. The light scattering data were recorded at Wacker Chemitronic, Burghausen. The oxide thickness has been determined with ellipsomtry.

7.2 Experimental results

LEED. The wafers are those misoriented samples, as described in section 6, that is a misorientation of 1,7° towards 211. As already described, the regularity in the direction of the step array and along the step edge could be measured independently by the appropriate scan direction of the spot profile. The more regular the step array is, the narrower is the probability distribution of the terraces. Its standard deviation from the average terrace width is therefore a measure for its regularity. For the regularity along the step edge the average length of straight edges has been taken. For the samples of group I the set of data was not complete for a full evaluation, the data, however, were sufficient to give the rank of the quality.

The results are shown in table 7.2.

T a b l e 7.2

Group	I	II	III	IV	V	VI
standard deviation (nm)						
from regular step array	-	1,6	1,0	1,4	1,8	1,0
rank fo quality	6	4	1	3	5	1
average length of straight edged	12	18	21	17	20	33
rank of quality	6	4	2	5	3	1
Electron spin resonance (spin / cm^2)	$2x10^{11}$	$5x10^{10}$	-	-	-	-
Electrical breakdown (MV / cm)	8,6	9,3	8,0	8,6	9,1	8,7
rank	4	1	6	4	2	3

The ESR measurements have been kindly made by E. Poindexter ET & DL, Fort Monmouth N. J. so far for the samples of the group I and II. The other measurements are in progress. His comments are, that the spin density is much lower than expected. An explanation cannot be given so far. The decrease from group I to II (annealing) is anyway very drastic. Electrical breakdown has been measured at Wacker-Chemitronic for two wafers out of each group. A typical example is shown for the wafers out of group II in fig. 7.1. The average breakdown field strength and a rank with respect to this quality is also shown in table 7.2.

7.3 Discussion

The summarized data of table 7.2 show a lot of interesting features: The wet-dry oxidation is superior in most properties, only with the breakdown it is not the best, here, however it had the lowest number of early failures. The

other surprising feature is, that the stray light intensity after oxidation does not correlate with the other properties, which cannot be explained so far. The other parameters, however, may be discussed together.

The influence of preoxidation (group II - V) is fairly small, it is not clear, if a systematic difference in quality is derived at all. Only the stray light has a strong effect.

The increased oxide thickness (group I - IV, II - III) increases the regularity and decreases the stray light. Only the extremely small breakdown of group III does not fit into this pattern.

The influence of annealing in dry N_2 at 1000°C after oxidation gives a very clear result (group I - II, IV - III). Both the structural homogeneity, the ESR spin density and the electrical breakdown show an improvement. Again the breakdown of group III is exceptional. Here the stray light is not affected at all.

As a surprise the wet-and-dry oxidation had a superior performance with respect to homogeneity. Although the stray light was high, th homogeneity is better than group II, III and V, which are closest in preparation due to annealing.

The present results for the first time combine quite a variety of structural and electrical methods for a study of defects at the Si/SiO_2 interface. Due to the novel evaluation procedures of high resolution LEED measurements the smoothness is characterizd in much more detail as before. The stray light measurements were not easily correlated here. It should be pointed out, however, that recent measurements of stray light with well defined angular variations are exactly correlated with LEED data, so that the roughness at the interface is described by the same geometric distribution from atomic distances up to several microns (publication in preparation, thesis completed). The electrical measurements include so far only ESR and breakdown field strength, which already show very relevant correlations. Since for the present series high resistivity silicon has been selected in favor of ESR, it was for the same reason not possible to do CV measurements or radiation damage studies. Therefore a new series with lower resistivity has been started.

8. Preparation of a study of a possible correlation of defects and radiation damage

A set of wafers have been prepared and oxidized with different oxidation parameters, so that a broad range of steps and other defects are expected. Since the oxidation was not done in our lab, we had to accept long delays to get a high quality oxidation at the level of industrial standard. So we ran out of time to do first the LEED measurements, which would be the prerequisite for radiation damage experiments by Dr. B. Mc Lean at the Harry Diamond Lab. As soon as we have funding, we will continue this series of measurements.

9. Summary and outlook

During the investigation the evaluation procedures for Spot Profile Analysis of LEED (SPA-LEED) has been developed to an unexpected high level, since due to the now available high resolution LEED systems qualitatively and quantitatively a big progress was possible. A surface is characterized now laterally up to more than 100 nm, completely new is the vertical analysis providing the rms roughness and the determination of the levels contributing to the interface. By a careful study of energy dependance also a second type of defect (other than steps) could be identified and separated.

With this evaluation procedure a precision analysis has been made for the (111) interface, showing in detail the effect of annealing.

Also the (100) interface now could be analyzed, to that also the technologically more relevant interface is now studied, showing in principle the same dependance.

The first big comparative study included besides LEED also ESR, optical stray light and electrical breakdown, showing the importance of the defect concentration (as determined by LEED) for electrical properties. The result suggest to look for more correlations between defect concentrations and other important electrical properties like radiation hardness or mobility in the inversion layer, which should be done in a subsequent study.

Figure Captions

Fig. 4.1a) Spot Profile for a SiO_2/Si(111) interface for out-of-phase condition. The solid line corresponds to the expected profile of a perfect crystal (instrumental broadening)
b) same as a) with the two Lorentzian shoulders shown as solid lines

Fig. 4.2a) Same as fig. 4.1 for in-phase condition. The existence of a broad shoulder indicates the presence of defect areas (other than steps)
b) same as a) with the broad Lorentzian shoulder as a solid line

Fig. 4.3a) Fraction of the integrated narrow shoulder I_s out of the total intensity VS energy,
b) same as a) for the broad shoulder

Fig. 4.4 Fraction of the integrated central spike intensity I_p out of the sum of I_p and I_s (= narrow shoulder), to determine the vertical structure

Fig. 5.1 Fraction of the integrated central spike out of the total intensity, calculated for a Si(100) as a 4 level system with same probability in each level. A is ratio of the form factors of the two non equivalent levels.

Fig. 5.2 Measured fraction of central spike for a Si(100) interface with an azimuthal incident direction, so that A = 1 (upper half) or A ≈ 0 (lower half)

Fig. 6.1 Area scan of a split diffraction spot due to a nearly regular step array for an energy close to an out-of-phase condition (both peaks nearly equal)

Fig. 6.2 Linear scan through the two peaks (with integration over the direction perpendicular to it) of fig. 6.1 for out-of-phase condition.

Fig. 6.3 Calculated terrace probability distribution for the Gamma-function with always the same average terrace width (Γ = 28) and different standard deviation.

Fig. 7.1 Breakdown of oxides on wafers of group II

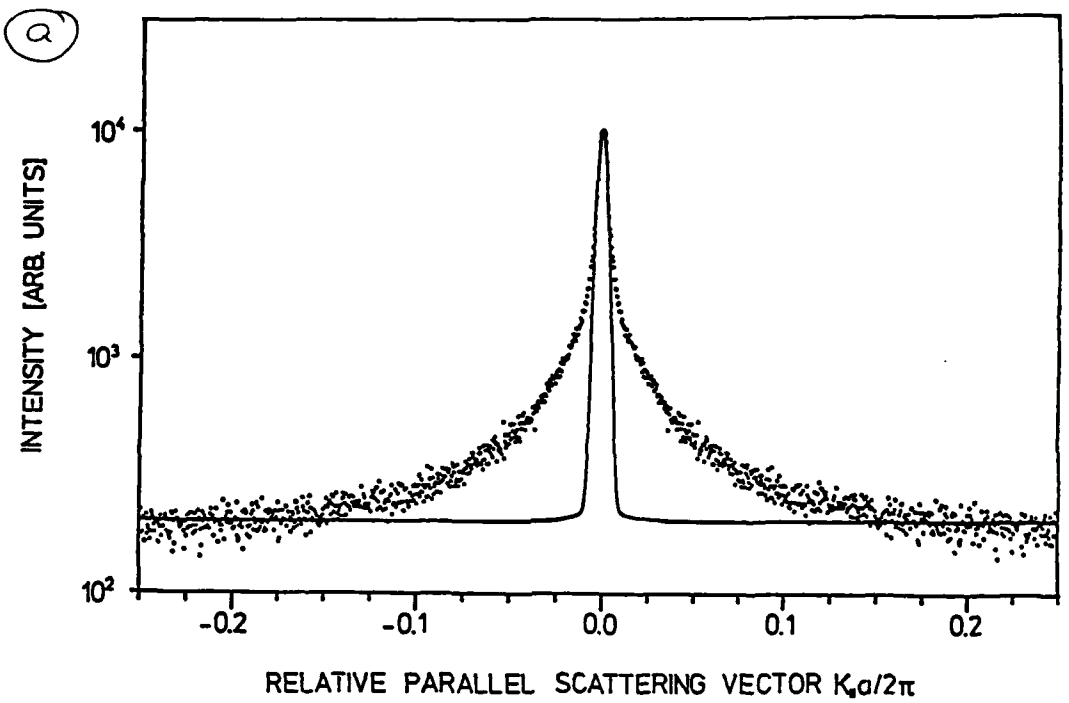
a
INTENSITY [ARB. UNITS]
10⁴
10³
10²
-0.2
-0.1
0.0
0.1
0.2
RELATIVE PARALLEL SCATTERING VECTOR K∥a/2π

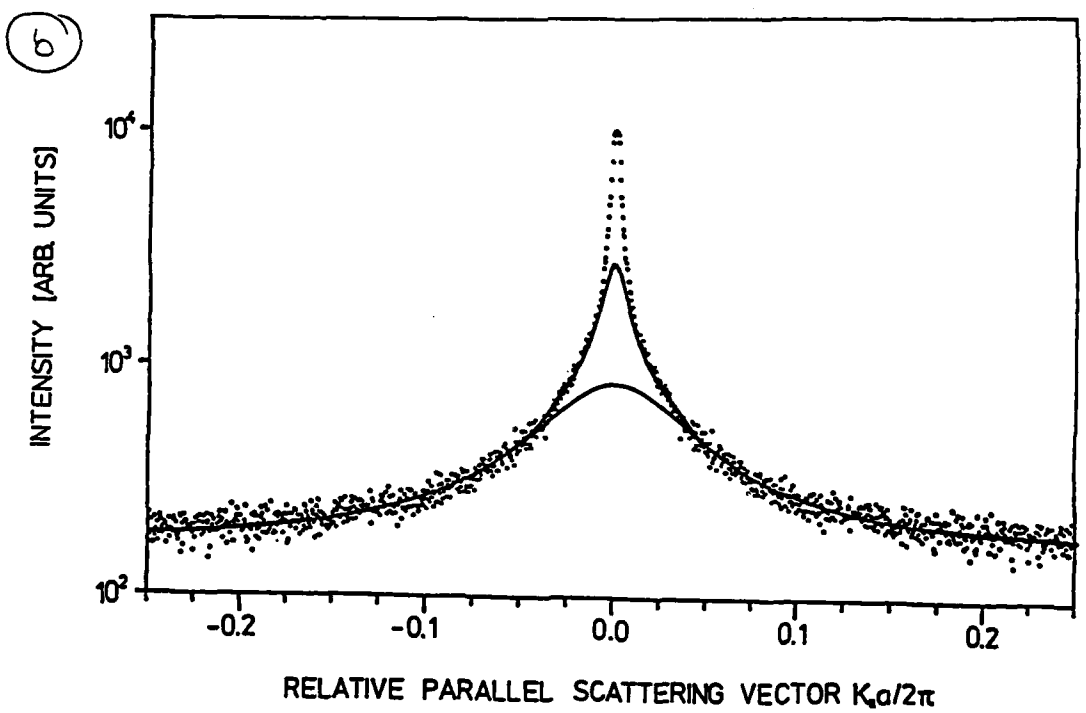
σ
INTENSITY [ARB. UNITS]
10⁴
10³
10²
-0.2
-0.1
0.0
0.1
0.2
RELATIVE PARALLEL SCATTERING VECTOR K∥a/2π

Fig. 4.1

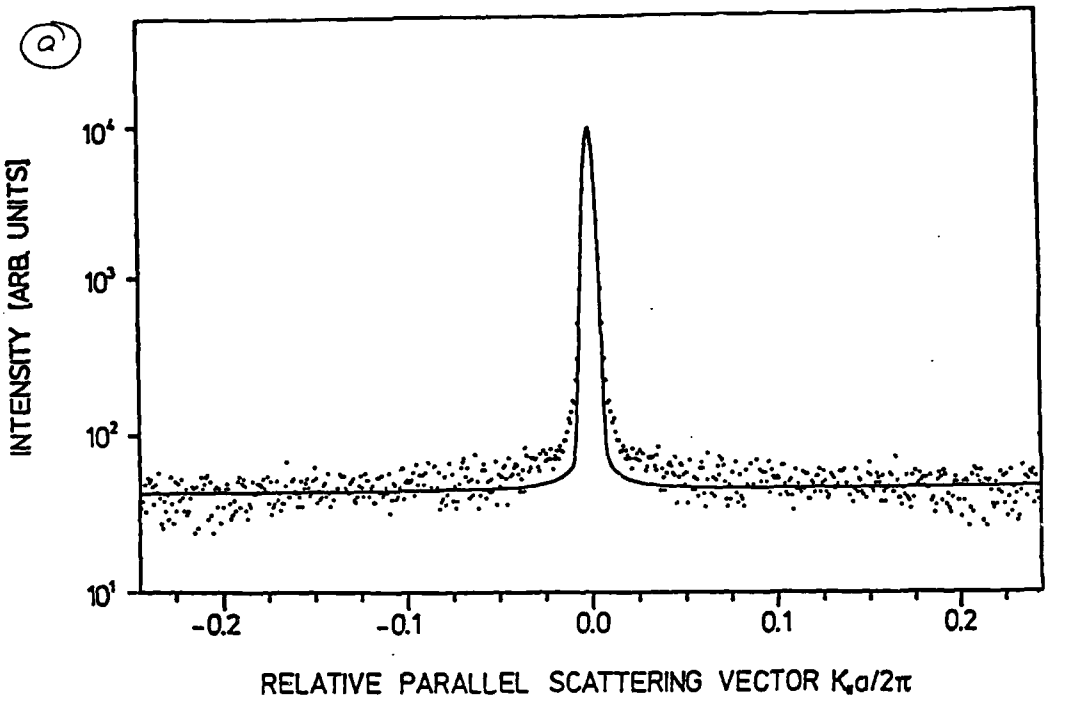
(a)
INTENSITY [ARB. UNITS]
10^4
10^3
10^2
10^1
-0.2
-0.1
0.0
0.1
0.2
RELATIVE PARALLEL SCATTERING VECTOR $K_{\parallel}a/2\pi$

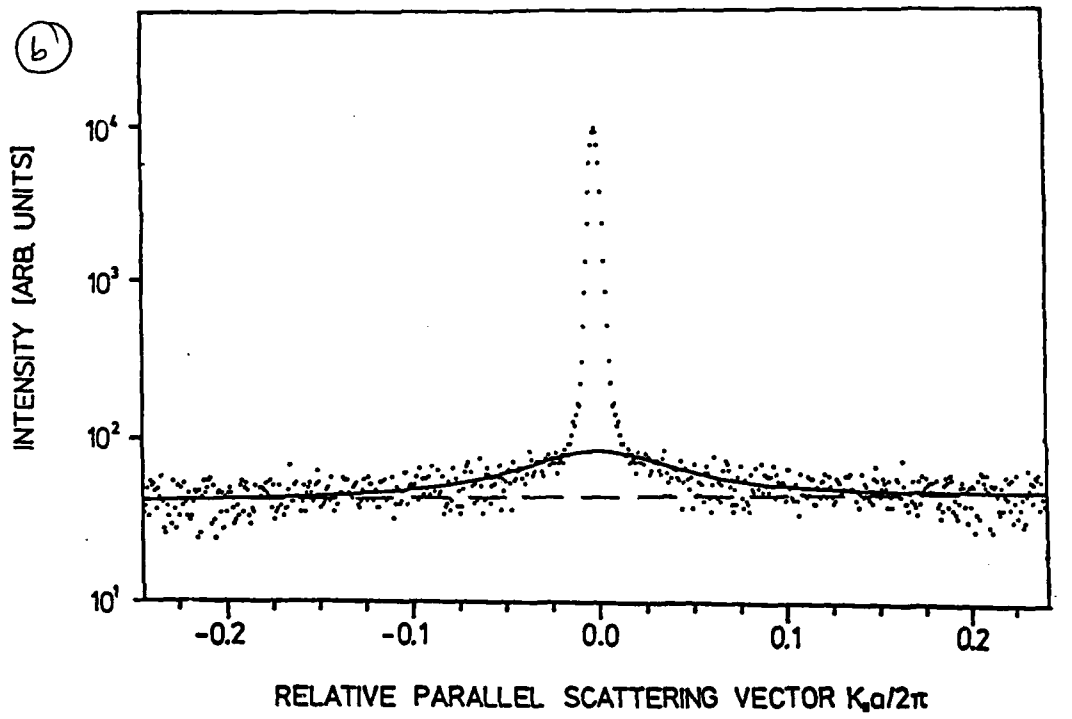
(b)
INTENSITY [ARB. UNITS]
10^4
10^3
10^2
10^1
-0.2
-0.1
0.0
0.1
0.2
RELATIVE PARALLEL SCATTERING VECTOR $K_{\parallel}a/2\pi$

Fig 4.2

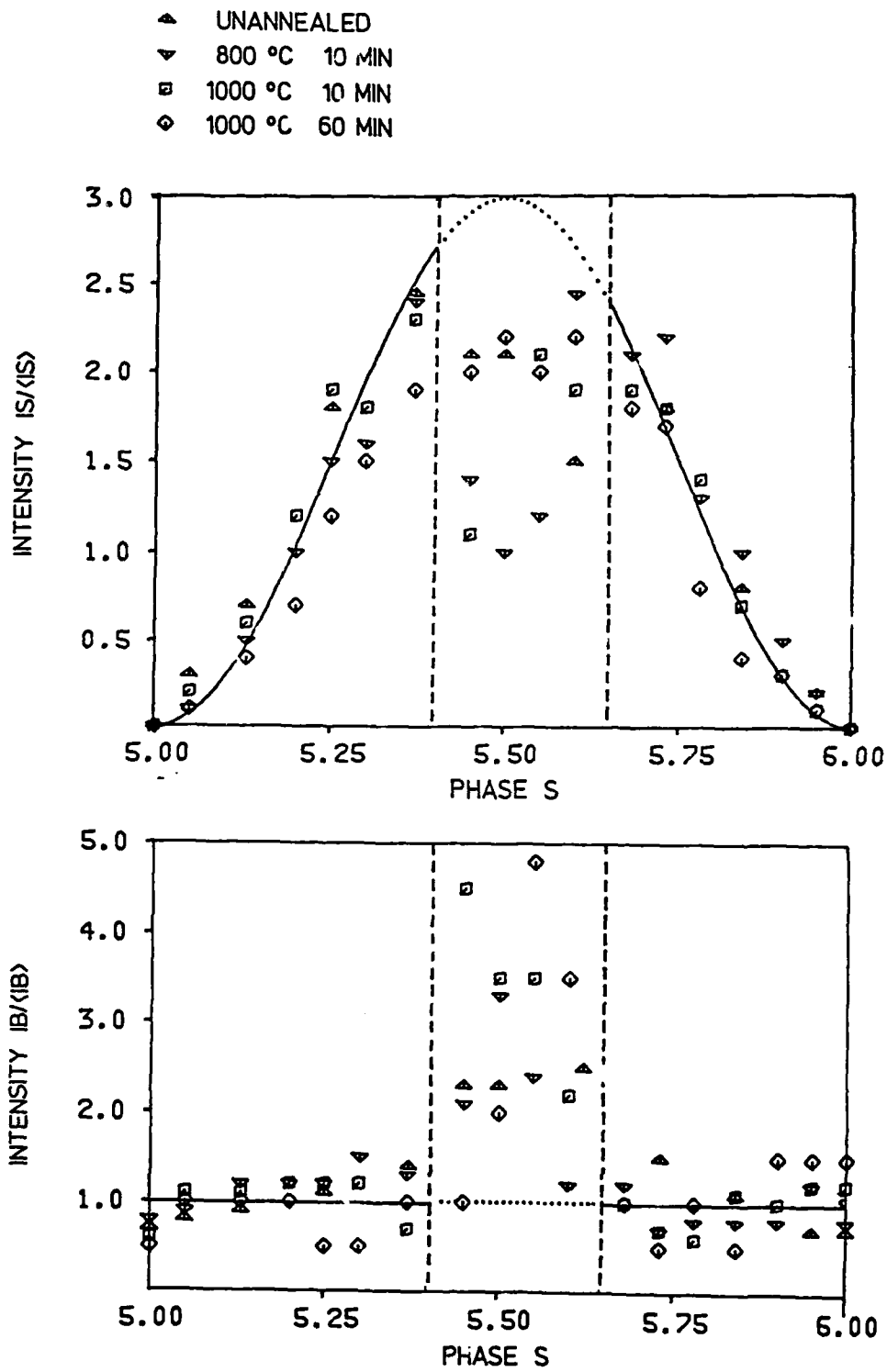
UNANNEALED
800 °C 10 MIN
1000 °C 10 MIN
1000 °C 60 MIN
INTENSITY IS/⟨IS⟩
3.0
2.5
2.0
1.5
1.0
0.5
5.00
5.25
5.50
5.75
6.00
PHASE S
INTENSITY IB/⟨IB⟩
5.0
4.0
3.0
2.0
1.0
5.00
5.25
5.50
5.75
6.00
PHASE S

Fig 4.3

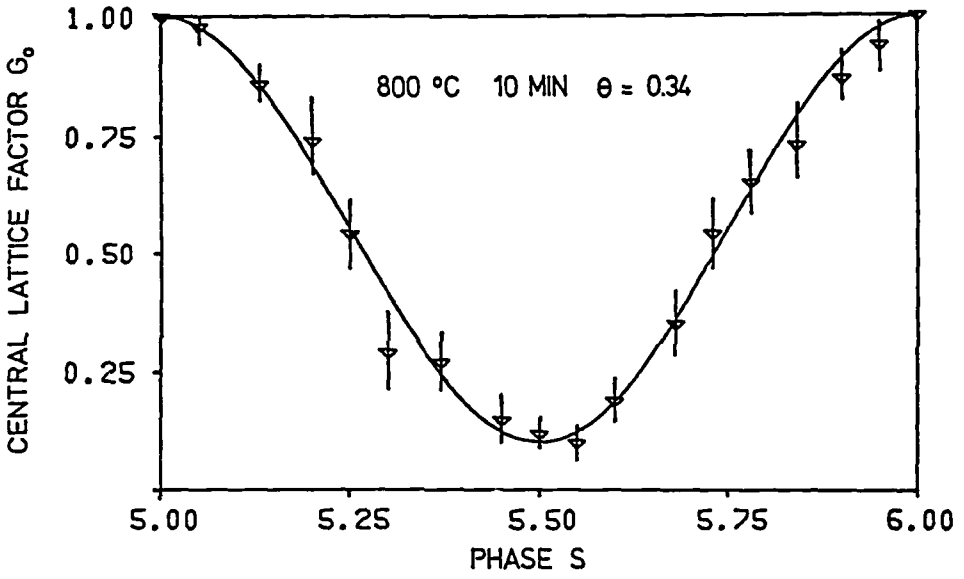
1.00
0.75
0.50
0.25
CENTRAL LATTICE FACTOR G_o
800 °C 10 MIN θ = 0.34
5.00
5.25
5.50
5.75
6.00
PHASE S

Fig 4.4

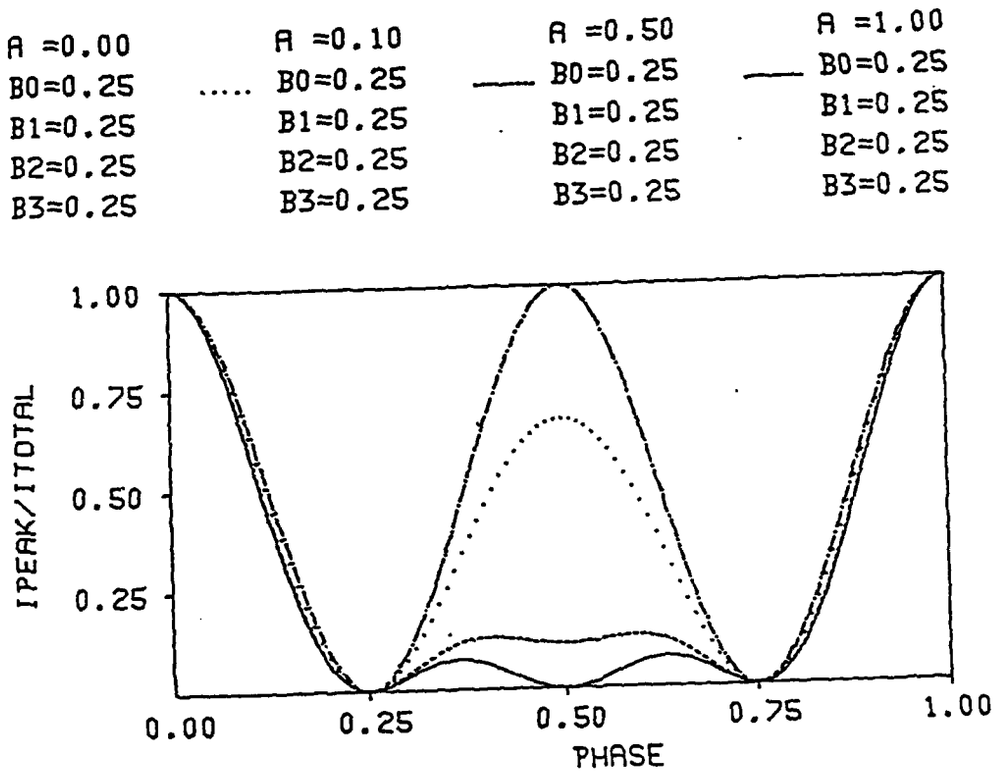
A =0.00
B0=0.25
B1=0.25
B2=0.25
B3=0.25
A =0.10
B0=0.25
B1=0.25
B2=0.25
B3=0.25
A =0.50
B0=0.25
B1=0.25
B2=0.25
B3=0.25
A =1.00
B0=0.25
B1=0.25
B2=0.25
B3=0.25
IPEAK/ITOTAL
1.00
0.75
0.50
0.25
0.00
0.25
0.50
0.75
1.00
PHASE

Fig. 5.1

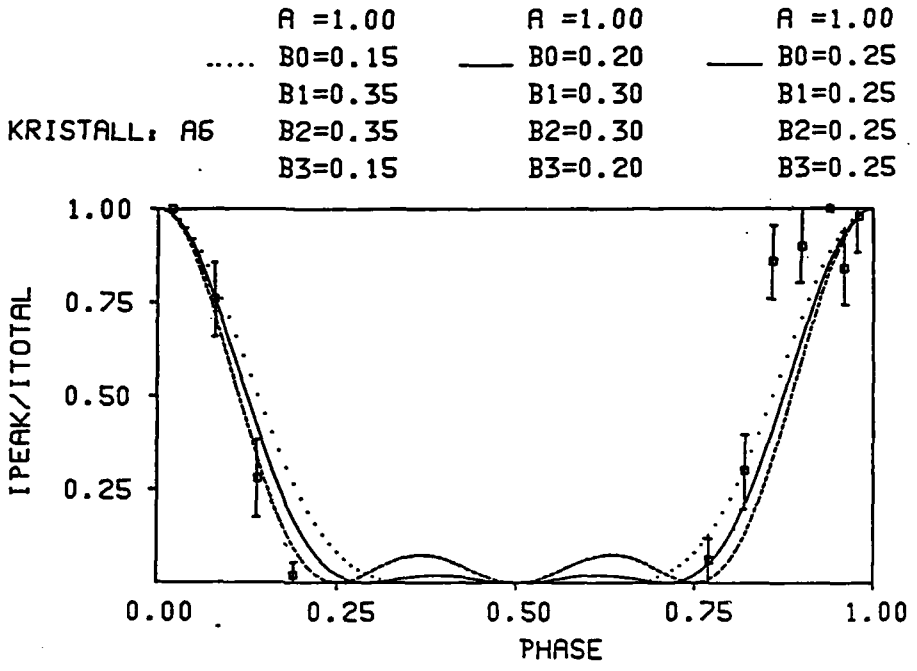
A =1.00
B0=0.15
B1=0.35
B2=0.35
B3=0.15
A =1.00
B0=0.20
B1=0.30
B2=0.30
B3=0.20
A =1.00
B0=0.25
B1=0.25
B2=0.25
B3=0.25
KRISTALL: A6
IPEAK/ITOTAL
1.00
0.75
0.50
0.25
0.00
0.25
0.50
0.75
1.00
PHASE

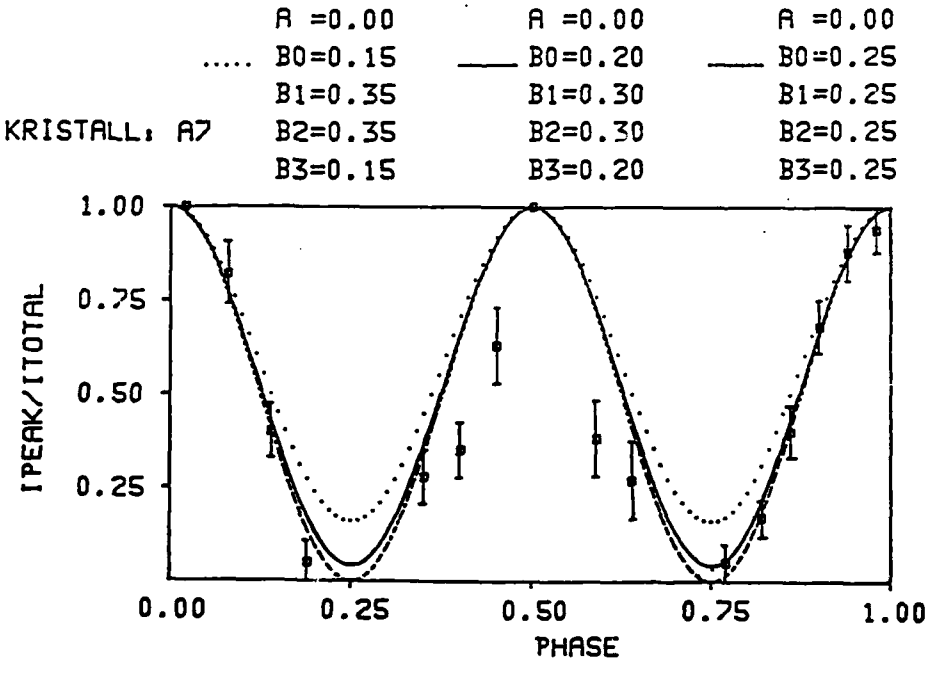
A =0.00
B0=0.15
B1=0.35
B2=0.35
B3=0.15
A =0.00
B0=0.20
B1=0.30
B2=0.30
B3=0.20
A =0.00
B0=0.25
B1=0.25
B2=0.25
B3=0.25
KRISTALL: A7
IPEAK/ITOTAL
1.00
0.75
0.50
0.25
0.00
0.25
0.50
0.75
1.00
PHASE

Fig 5.2

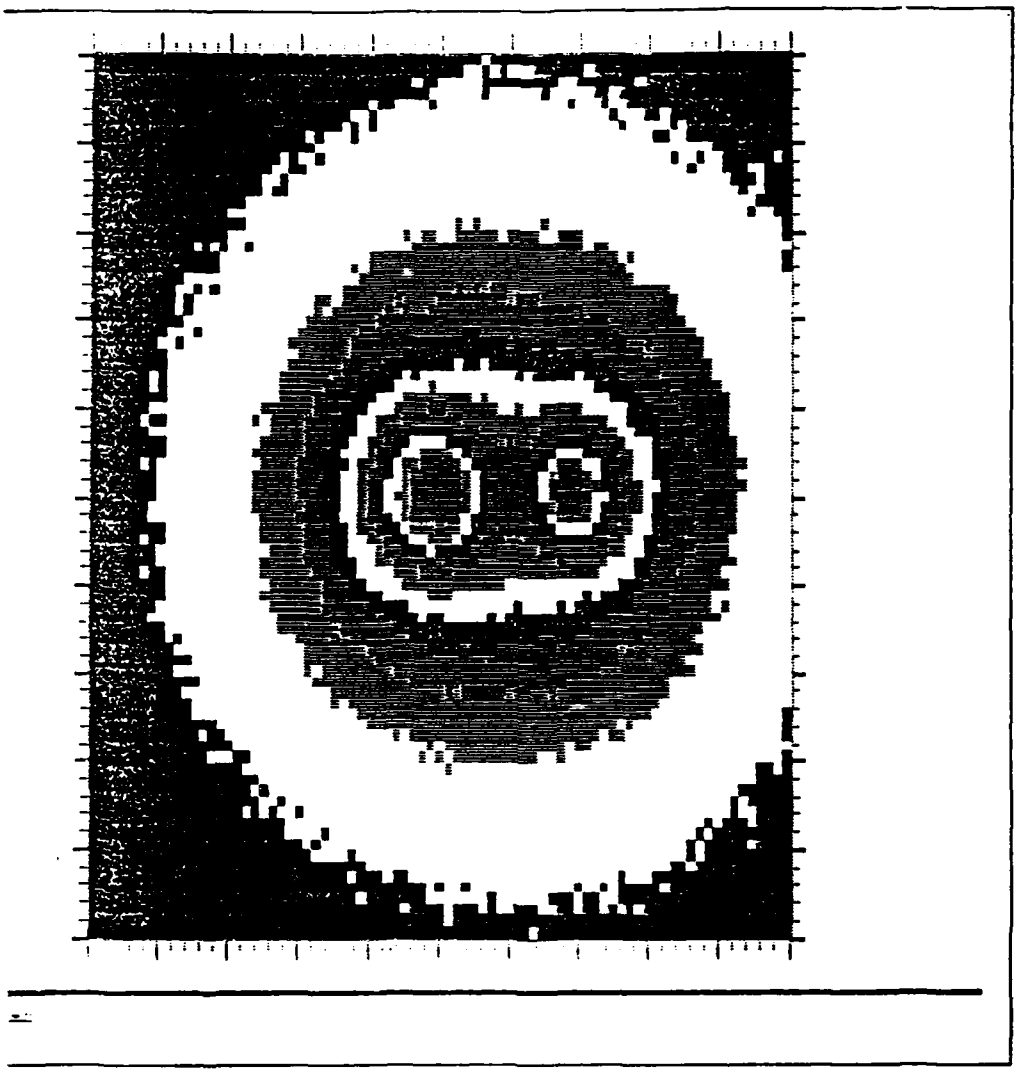

Fig. 6.1

INTENSITY [ARB. UNITS]
RELATIVE PARALLEL SCATTERING VECTOR $K_{\parallel}a/2\pi$
x10^3
100.00

Fig. 6.2

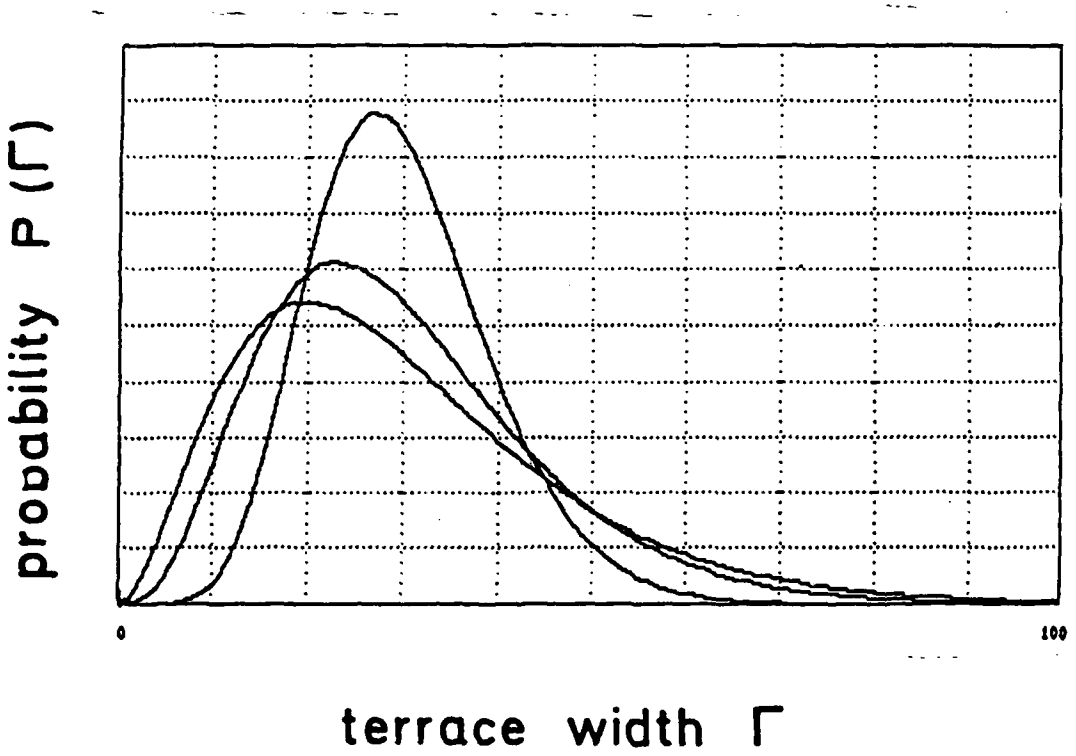

Fig. 6.3

BREAKDOWN OF MOS

7 Oct 1987

Sample	Oxth[Å]	Area[cm^2]	Def.Dens.[cm^-2]	Ed[MV/cm]	Ed1[MV/cm]
NANZLER7_6	365	.0014	16	9.5	9.7
NANZLE12_6	360	.0014	124	9.2	9.8

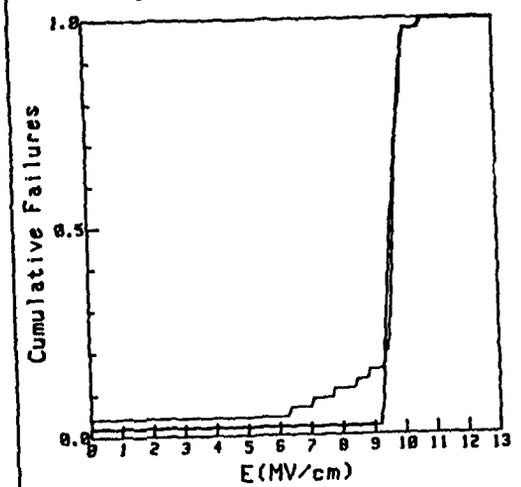

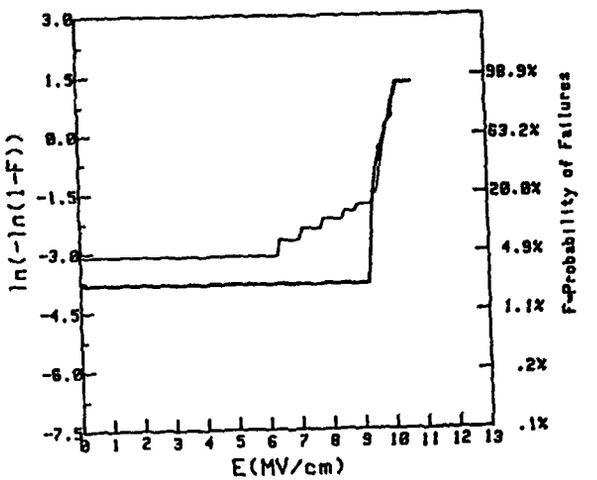

HENZLER-SCHEIBEN GRUPPE II (IU-MESSUNG)

WACKER CHEMITRONIC FOU